



## Various Approaches to Thermodynamic Optimization of a Hybrid Multi-effect Evaporation with Thermal Vapour Compression and Reverse Osmosis Desalination System Integrated to a Gas Turbine Power Plant

S. E. Shakib<sup>\*a</sup>, M. Amidpour<sup>b</sup>, A. Esmaielj<sup>b</sup>, M. Boghrati<sup>a</sup>, M. M. Ghafurian<sup>c</sup>

<sup>a</sup> Department of Mechanical Engineering, Bozorgmehr University of Qaenat, Qaen, Iran

<sup>b</sup> Faculty of Mechanical Engineering, K.N. Toosi University of Technology, Tehran, Iran

<sup>c</sup> Department of Mechanical Engineering, Faculty of Engineering, Ferdowsi University of Mashhad, Mashhad, Iran

### PAPER INFO

#### *Paper history:*

Received 14 December 2018

Received in revised form 30 January 2019

Accepted 07 March 2019

#### *Keywords:*

Optimal Design

Multi-effect Evaporation with Thermal

Vapour Compression

Reverse Osmosis

Desalination

Thermodynamic Approach

### ABSTRACT

This paper investigates the simulation of a hybrid desalination system composed of multi-effect evaporation with thermal vapour compression desalination (METVC) and reverse osmosis (RO) plant. The hybrid desalination system is also integrated with a gas turbine power plant through a heat recovery steam generator (HRSG). First, a comprehensive Thermodynamic model for HRSG, METVC, and RO are developed for predicting thermal behaviour of hybrid desalination system. Depending on the interconnection between input and output streams of METVC and RO, six configurations are proposed, and their results are compared in two different scenarios. In the first scenario, METVC desalination production is fixed at its maximum capacity of 70000 m<sup>3</sup>/day. The heat potential of power plants is fully extracted at maximum capacity of production of METVC. In the second scenario, METVC desalination production is not fixed. The limitation on the total production of the desalination plant (METVC+RO) is imposed as a constraint to the optimization problem. The results show that, regardless of the scenario under consideration, configuration 1 (the outlet water of the cooling system in METVC has been used for the feed water of the RO system) has the minimum energy consumption as well as maximum exergy efficiency.

*doi:* 10.5829/ije.2019.32.05b.20

## 1. INTRODUCTION

With population growth and industrial demands for drinking water, many technologies have been developed to make fresh water from brackish and seawater. However, the quantity and quality of fresh water, process and economic efficiency, and energy consumption are key factors to prefer the type of convenient technology. Furthermore, the efficiency of industrial processes and thermal plants, as well as energy recovery, is highly regarded due to the decline of fossil fuel resources [1]. Applying thermal desalination technologies can be considered as one of the most beneficial methods in recovery of waste heat of power plants. Multi-stage flash (MSF) desalination and multi-effect evaporation (MED) with thermal vapour compression (METVC) are the most common types of thermal desalination systems.

Comparative study of METVC and MED desalination systems shows the advantages of METVC desalination system in longer operation life and lower capital cost, scaling rates, corrosion, and pumping power consumption [2]. On the other hand, the rate of development in reverse osmosis (RO) units reduces the high cost of desalinated water compared to the thermal methods such as MSF [3, 4].

MED and METVC desalination systems have been investigated technically and theoretically in recent years. For instance, economic assessment [5–7], energy cost [8], hybrid thermal desalination structures [9], simulation of MED–TVC units [10], optimal operation schemes [11], exergy analysis and thermoeconomic cost [12], and Techno-economic analysis [13] have been studied by some researchers.

The rate of development in reverse osmosis (RO)

\*Corresponding Author Email: se.shakib@buqaen.ac.ir (S. E. Shakib)

units reduces the high cost of desalinated water compared to the thermal methods such as MSF [3, 14]. A hybrid desalination plant for recovering heat potential of power plant (METVC) and a RO unit enhances the thermal efficiency and reduces the cost of production. Many researches have been investigated the hybrid desalination plants from several aspect of views. Awerbuch et al. [15], Altmann [16], and Al-Mutaz [17] studied MSF and RO desalination technologies. At the same time, a few researchers have evaluated METVC+RO desalination. La Bar et al. [18] and Kamal [19] studied RO and LTMETVC<sup>1</sup> desalination technologies in the context of power plants in the US. The performance of each of these desalination technologies was economically analysed in two ways, solely and hybrid.

Muginstein et al. [20] studied RO and METVC desalination technologies related to combined cycle power plants. They investigated two scenarios of dual purpose plants, METVC and RO technologies. In METVC technology, the capacity of daily dispatch limited the output of desalination plant. The RO unit received its essential energy from electricity production of power plant.

Cardona et al. [21] studied a hybrid METVC+RO desalination unit. The METVC unit received the essential thermal energy from a diesel generator. The hybrid system reduced the cost of fresh water and production of carbon dioxide by 8% and 30%, respectively.

Messino et al. [22] conducted a similar study to the one conducted by Cardona et al. [21]. The only difference lay in the absence of thermal coupling between METVC and RO. The drinking water was mixed to achieve the quality.

Zak et al. [23] reviewed thermal desalination, seawater reverse osmosis (SWRO), and co-generation of power and water in the context of their use in hybrid plants. They also reviewed the design and economics of hybrid desalination plants. In another study, Iaquaniello et al. [24] proposed an integration of CSP with multi-effect distillation (MED) and RO desalination processes. The MED is powered by low temperature exhaust steam delivered from a steam turbine, while the RO is powered by electricity produced by the same steam turbine and gas turbine integrated as a thermal backup system.

Mokhtari et al. [25] presented a design of a Gas Turbine, MED, and RO to provide electrical power and water for Bashagard County in the south of Iran. They selected an MED unit to be combined with Siemens gas turbine plant, but due to the high flow rates of the MED reject, a RO system was used the reject of the MED system as the feed water. In a similar study, Sadri et al. [26] presented a mathematical model for the hybrid MED-TVC+RO system. The proposed system utilized the reject of RO as the feed water of MED-TVC and the

final product was obtained by mixing the RO and MED-TVC products.

As described above, the simultaneous use of thermal and osmosis technologies has gained wide acceptance in the past few years, a few numbers of which have focused on METVC+RO plants as before-mentioned. Nevertheless, only some studies in this regard have focused on general issues since their results have not been able to present a general conclusion.

To be more precise, no comprehensive research has considered the simultaneous combination of METVC and RO. In fact, the gap is obvious in studying the integration method of these two desalination systems and various configuration optimizations. In other words, the basic challenge is how the METVC and RO should be combined with each other. Considering the limitations of the mentioned studies and in continuation of previous researches [27, 28], in this study, several possible configurations of METVC and RO were first proposed and then the optimum configurations of METVC and RO with HRSG and the gas turbine cycle were investigated to achieve the optimum amounts of the key thermodynamic parameters. At the same time, HRSG was modelled and optimized, simultaneously. The interaction of METVC and RO plants is studied as several configurations in various scenarios. Consequently, the optimum integration of METVC+RO hybrid desalination with a gas turbine cycle was investigated by two approaches with respect to total product capacity.

## 2. SYSTEM DESCRIPTION

The system under consideration comprises a gas power plant, a recovery boiler, METVC desalination, and RO desalination. Nation Figure 1 shows schematic diagram of the desalination system. The integration between heat recovery steam generator (HRSG), METVC, and RO desalination units is discussed here.

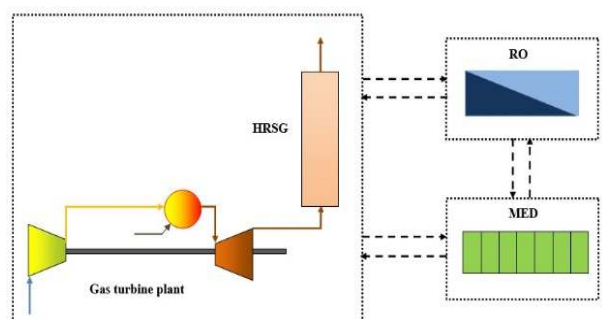


**Figure 1.** A schematic diagram of gas power plant, HRSG, METVC desalination, and RO desalination

<sup>1</sup> Low Temperature Multi Effect Desalination

### 3. THERMODYNAMIC ANALYSIS

**3.1. Heat Recovery Steam Generator (Hrsg)** A HRSG unit recovers the heat potential of high temperature flue gas of turbine exhaust. Furthermore, HRSG generates the essential steam for desalination system.

Figure 2 shows the schematic diagram of the HRSG applied to the power plant. HRSG is composed of an economizer and an evaporator to generate essential motive steam for METVC unit. The required motive steam is assumed to be saturated. Therefore, the boiler does not need any super heater section.

In the economizer, according to theoretical concepts, the state of water changes into saturated liquid. However, in actual operating conditions, vapour formation of outlet water at the end of the economizer, are the major restrictions for water state changing. So, the temperature of outlet water of the economizer is lower than the saturated temperature in actual process. This difference temperature is introduced by the approach point. On the other hand, the pinch point minimize the difference between the gas temperature of the evaporator outlet and the saturation temperature. Therefore, a lower pinch point results a HRSG with a large heat transfer surface. Thus, increasing the pinch point temperature results a reduction in the essential heat transfer surface. Eventually, the pinch point should be considered from both thermodynamic and economic points of view. Therefore, both the pinch point and the approach point are included in the modelling. The HRSG model is comprehensive enough to forecast the real case behaviour and simulate thermal performance, which is presented completely in reference [29] by the authors. Table 1 shows the verification of the HRSG model.

**3.2. Metvc Modelling** Figure 3 shows the schematic diagram of METVC plant, by applying mass and energy conservation laws to the evaporators, steam ejector, flash boxes, and condenser, a mathematical model is developed. The mathematical model evaluates

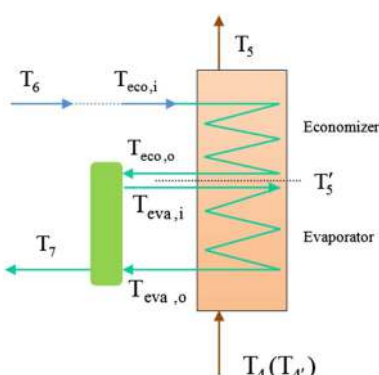


Figure 2. Heat recovery steam generator

TABLE 1. Verification of HRSG mode

parameter	Ref. [29]	present model
$m_g$ (kg/s)	28.98	28.98
$T_1$ (°C)	838.706	838.706
P (bar)	14.84	14.84
$d_i$ (m)	0.045	0.045
$h_f$ (m)	0.01905	0.01905
L (m)	3.353	3.353
$T_2$ (°C)*	480.928	476.213
$U$ (w/m <sup>2</sup> K)*	42.019	40
$\Delta P_g$ (pa)*	846.879	1032.623
$Q$ (Mw)*	11.606	11.394

the thermal performance and METVC essential heat transfer area.

The following assumptions are considered for the desalination system:

- METVC vapour is free of salt in each effect.
- No heat loss is found in the desalination or the environment.
- Final reject salinity is assumed 70,000 ppm in METVC plant.
- The heat transfer area is the same for each evaporator (2 to N).
- The temperature difference is initially the same for all effects, where  $T_1$  and  $T_N$  are the the temperatures of first and the last effect, respectively:

$$\Delta T = \frac{T_1 - T_N}{N-1}. \quad (1)$$

$$T_1 = T_s - \Delta T. \quad (2)$$

$$T_{i+1} = T_i - \Delta T. \quad (3)$$

The mass conservation of Water and salt for the first effect and effects 2 to N are as follow:

$$B_1 = F - D_1. \quad (4)$$

$$B_i = F + B_{i-1} - D_i. \quad i = 2, \dots, N \quad (5)$$

$$x_1 = \frac{F}{B_1} x_f. \quad (6)$$

$$x_i = \frac{F}{B_i} x_f + \frac{B_{i-1}}{B_i} x_{i-1}. \quad i = 2, \dots, N \quad (7)$$

where F, B, and D represent salty water flow rate, waste water, and drinking water (kilogram per second), respectively. x displays salinity percentage, and i sub-index indicates the step.

The first-effect motive steam is supplied by the heat recovery steam generator. Therefore, the energy balance equation can be written as follows for the first effect:

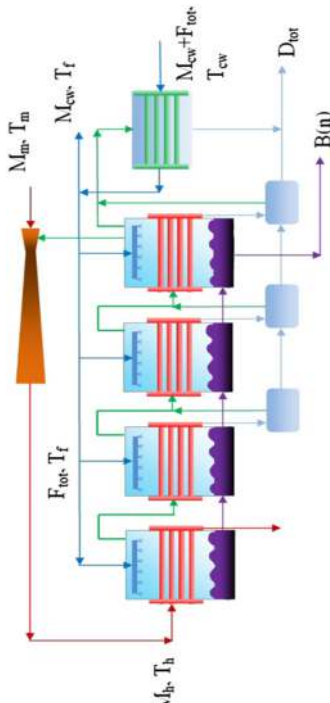


**Figure 3.** Four-effects thermal vapour compression desalination (METVC)

$$D_1 = \frac{1}{L_1} [M_s L_s - F C_p (T_1 - T_f)]. \quad (8)$$

At the same time, vapour is generated by two mechanisms in effects 2 to N: boiling and flashing. The outlet brine of each effect enters the next effect and a small amount of vapour is associated for METVC due to dropping pressure. Another small quantity of vapour is associated for METVC in the flash box due to the flashing of distillate condensed in the previous effect. The mass flow rate of vapour for METVC in the flash box is calculated by the following equation [28].

$$D'_i = D_{i-1} C_p \frac{T_{v,i-1} - T_i'}{L_i}. \quad (9)$$

So, the energy balance equation of effects 2 to N can be written as:

$$D_i = \frac{1}{L_i} [(D_{i-1} + D'_{i-1}) L_{i-1} - F C_p (T_i - T_f) - B_{i-1} C_p \Delta T]. \quad (10)$$

The amount of total product of fresh water can be calculated as:

$$M_d = \sum_{i=1}^N D_i \quad (11)$$

The cooling water flow rate is determined by the following equation:

$$M_{cw} = \frac{(D_N + D'_N - M_{ev}) L_s}{C_p (T_f - T_{cw})} - M_f. \quad (12)$$

The heat load of the evaporator, condenser, and the specific heat transfer area can be calculated by the following equations, respectively:

$$A_1 = \frac{M_s L_s}{U_{e1} (T_s - T_1)}. \quad (13)$$

$$A_i = \frac{(D_{i-1} + D'_{i-1}) L_{i-1}}{U_{ei} \Delta T}, \quad i = 2, \dots, N \quad (14)$$

$$A_c = \frac{(D_N + D'_N) L_N}{U_c LMTD_e}. \quad (15)$$

$$a = \frac{\sum_{i=1}^N A_i + A_c}{D_{tot}} \quad (16)$$

One of the most important characteristics of thermal desalination is the performance ratio (PR), the ratio of the mass of the produced fresh water to that of the consumed motive steam:

$$PR = \frac{M_d}{M_m} \quad (17)$$

The model developed by reference [30] is used for the steam jet ejector. Tables 2 shows the verification of the METVC model.

### 3.3. RO Desalination System

Figure 4 shows a schematic diagram of the RO desalination system. There are three main parts: high pressure feed pump, pressure vessel, and energy recovery unit to decrease pump consumption power.

**TABLE 2.** Verification of METVC model

parameter	n=4		n=5	
	Ref. [31]	present model	Ref. [31]	present model
D (kg/s)	0.7	0.7	0.88	0.89
F (kg/s)	4.81	5.03	5.02	5.23
A <sub>tot</sub> (m <sup>2</sup> )	222	219	283	279
PR	6.14	6.05	7.72	7.80

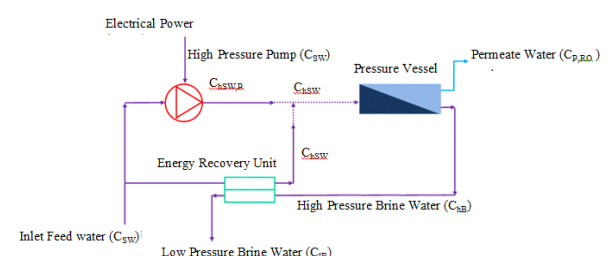


**Figure 4.** Thermo-economic model of RO unit

The pressure vessel comprises some RO membrane arrays. The number of these arrays ranges from 5 to 8 based on water concentration.

The assumptions regarding the model RO desalination system are as follows:

- There is no chemical reaction.
- The process is performed at a constant temperature.
- The system is in a steady state.

Mass continuity equations are presented below for water and salt:

$$Q_f = Q_c + Q_p \quad (18)$$

$$Q_f C_f = Q_c C_c + Q_p C_p \quad (19)$$

where  $Q$  is the volumetric flow rate ( $\text{m}^3/\text{s}$ ), and subscripts f, c, and p are feed water, brine water, and permeate water, respectively. The following equation is employed to calculate water and salt fluxes [32, 33]:

$$Q_p = J_w A \quad (20)$$

$$J_w = A_w (\Delta P - \Delta \pi) \quad (21)$$

$$J_s = B_s (C_m - C_p) \quad (22)$$

where A is the effective surface of RO membrane arrays ( $\text{m}^2$ ),  $\Delta P$  is the pressure difference between feed water and final production,  $\Delta \pi$  is the pressure difference in the membrane array, and  $A_w$  and  $B_s$  refer to the coefficients of water and solute permeability. The following equation is used to calculate them [34]:

$$A_w = 4.5 \times 10^{-7} \times \exp \left( 8.6464 \left( \frac{T_{f-RO} - 293}{293} \right) - 0.0028 P_f \right) \quad (23)$$

$$B_s = 6.8 \times 10^{-9} \times \exp \left( 14.648 \left( \frac{T_{f-RO} - 293}{293} \right) \right) \quad (24)$$

where  $T_{f-RO}$  is the feed water temperature. Applying the Filmtec SW30HR-380 module to this approach and concentration distribution, the following experimental correlation is achieved [32, 35]:

$$\pi = 0.9524 C^2 + 81633 C - 236143 \quad (25)$$

The effective area is  $35 \text{ m}^2$  for this type of module. Using the following equation, the osmosis pressure difference is achieved:

$$\Delta \pi = 0.9524 (C_m^2 - C_p^2) + 81633 (C_m - C_p) \quad (26)$$

According to concentration polarization:

$$(C_m - C_p) = (C_b - C_p) \exp \left( \frac{J_w}{k} \right) \quad (27)$$

where  $k$  is the mass transfer coefficient and subscript b refers to bulk. By substituting Equation (24) in Equation (23), the following equation is achieved:

$$\begin{aligned} \Delta \pi = & 0.9524 \left[ (C_b - C_p) \exp \left( \frac{J_w}{k} \right) \right] \\ & \left[ (C_b - C_p) \exp \left( \frac{J_w}{k} \right) + 2C_p \right] \\ & + 81633 \left( C_b - C_p \right) \exp \left( \frac{J_w}{k} \right) \end{aligned} \quad (28)$$

The bulk concentration is linearly related to feed water and brine water concentrations:

$$C_b(x) = C_f + \left( \frac{C_c - C_f}{L} \right) x \quad (29)$$

In the above-mentioned equation, x and L refer to the distance (m) and length of element (m), respectively. The following equation is employed to calculate the final product concentration [32]:

$$C_p = C_b \left( \frac{B_s}{J_w + B_s} \right) \quad (30)$$

The mass transfer coefficient is achieved in the channel of spiral wound modules as follows [34]:

$$Sh = 0.664 k_{dc} Re^{0.5} Sc^{0.33} \left( \frac{2d_h}{l} \right) \quad (31)$$

$$Sh = \frac{k d_h}{D} \quad (32)$$

$$Re = \frac{\rho d_h u}{\mu} \quad (33)$$

$$u = \frac{Q_b}{w h_{sp} \epsilon} \quad (34)$$

In the above equations, Sh, Sc, and Re are dimensionless numbers—Sherwood, Schmidt, and Reynolds. D, u, and  $Q_b$  are the diffusion coefficient of salt ( $\text{m}^2/\text{s}$ ), mean fluid velocity, and average volumetric flow rate in the pressure vessel, respectively. The amounts  $k_{dc}$ , w, l,  $h_{sp}$ ,  $d_h$ , and  $\epsilon$  are presented in Table 3.

**TABLE 3.** The specifications of Filmtec SW30HR-380 [14]

Parameter	Amount
$k_{dc}$	1.05
$d_h(\text{m})$	$8.126 \times 10^{-4}$
$l(\text{m})$	$2.77 \times 10^{-3}$
$h_{sp}(\text{m})$	$5.93 \times 10^{-4}$
$\epsilon$	0.9
$A'$	7.38
N	0.34

The mean volumetric rate of flow is calculated as follows:

$$Q_b = \frac{Q_f + Q_c}{2}. \quad (35)$$

The pressure drop is calculated as fluid passes in the membrane.

$$\Delta P_L = \frac{\alpha^2 L C_{td}}{2d_h}. \quad (36)$$

$$C_{td} = \frac{A'}{Re^n}. \quad (37)$$

$$\Delta P = (P_f - \Delta P_L) - P_p \quad (38)$$

The mentioned equations form a non-linear system of equations can be solved using the input values. To achieve the final values of the flow rate, concentration of permeate, and brine water, this system of equations must be solved for each module in the pressure vessel. The input of the next module is the output of the previous module. Thus, the final volumetric flow rate and concentration of permeate water are achieved as follows:

$$Q_p = \sum_{j=1}^n Q_{p,j}. \quad (39)$$

$$C_p = \frac{\sum_{j=1}^n C_{p,j} Q_{p,j}}{Q_p}. \quad (40)$$

The specific consumption of RO desalination system is calculated as follows:

$$sE_{Ro} = \frac{Q_f P_f (\eta_{pump})^{-1} - Q_{ers} P_{ers} (\eta_{ers})^{-1}}{Q_p}. \quad (41)$$

Table 4 shows the product purity verification of the present model for  $\Delta P = 63$  bar.

### 3.4. Hybrid (Metvc+Ro) Desalination Plants

The following points need to be considered while connecting

**TABLE 4.** Product purity verification of present model of RO system for  $\Delta P = 63$  bar

Module No.	Present model	Experimental results [35]	Theoretical results [35]
1	201	195	205
2	220	230	233
3	251	250	263
4	289	285	298
5	333	312	335
6	383	369	375

METVC and RO desalination units:

- A rise in the RO feed water temperature leads to increased passage of mass flow rate through membrane modules.
  - The cost and concentration of the fluid flows must be calculated from one module as a feed fluid to the next.
  - The required electrical energy of the RO units is supplied by the gas turbine power plant.
- Six configurations were proposed Based on the inputs and outputs of RO and METVC desalination:

#### 3.4. 1. Configuration 1

Figure 5 shows the schematic diagram of configuration 1. The feed water of the RO system is the outlet water of the cooling system in METVC desalination. The main attributes of this configuration are higher temperature of cooling water related to feed water and its similar concentration to that of seawater.

#### 3.4. 2. Configuration 2

The temperature of production of METVC and MSF units is significantly higher than feed water temperature. The higher temperature of production causes many problems in water transfer. In RO units, all the processes occur at a constant temperature. Figure 6 shows the schematic diagram of configuration 2. According to Figure 6, the RO feed water gain heat passing through a heat exchanger from METVC production. So, the temperature of RO feed water increased.

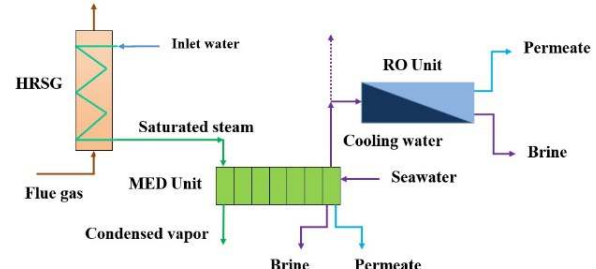


**Figure 5.** Schematic diagram of METVC+RO hybrid system, Configuration 1

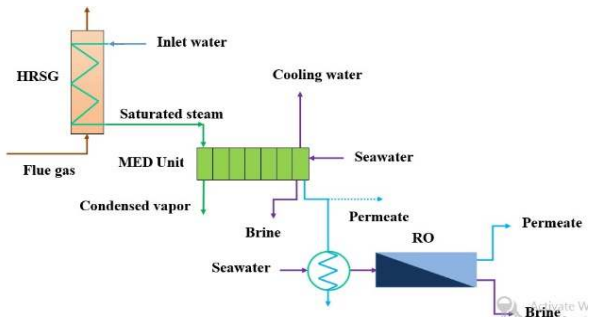


**Figure 6.** Schematic diagram of METVC+RO hybrid system, Configuration 2

**3. 4. 3. Configuration 3** Figure 7 shows the schematic diagram of configuration 3. The difference between configuration 3 and configuration 2 lies in the inlet of heat exchanger. There is a heat transfer between the feed water of RO unit and the brine water of METVC in a heat exchanger.

**3. 4. 4. Configuration 4** Figure 8 shows the schematic diagram of configuration 4. The brine water of METVC is directly utilized as feed water of the RO unit in configuration 4. Partial or full mixture of METVC brine water with sea water leads to a desirable concentration of RO unit feed water. The higher concentration of RO unit feed water affected the economic aspects of the system.

**3. 4. 5. Configuration 5** Figure 9 shows the schematic diagram of configuration 5. Unlike the previous configurations, the brine water of the RO unit is mixed with seawater and utilized as feed water in the METVC system. The more efficient performance of METVC system in desalination of higher concentration of brine water, is the advantage of configuration 5. The temperature of METVC feed water is equal to seawater temperature.

**3. 4. 6. Configuration 6** In the configuration 6, the METVC+RO system are separately investigated and there is no mechanical and thermal connection between METVC and RO units.

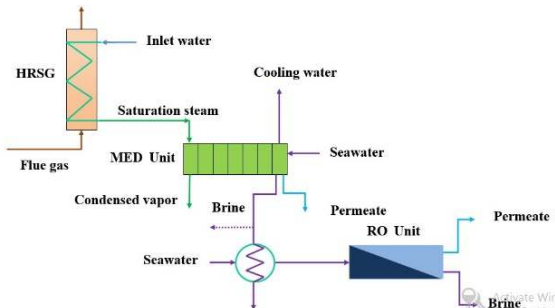


**Figure 7.** Schematic diagram of METVC+RO hybrid system, configuration 3

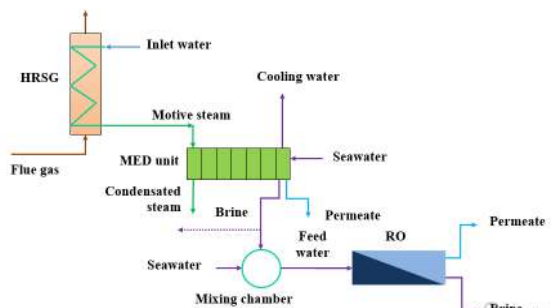


**Figure 8.** Schematic diagram of METVC+RO hybrid system, configuration 4

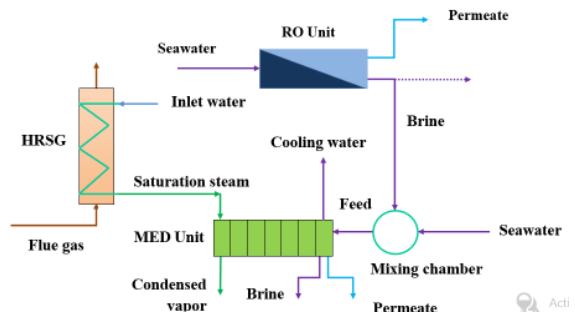


**Figure 9.** Schematic diagram of METVC+RO hybrid system configuration 5

#### 4. EXERGY ANALYSIS

Specific exergy (exergy of unit mass) is the summation of physical, kinetic, potential, and chemical exergy in the absence of nuclear, magnetic, and electrical effects and surface tension [36]:

$$e = e^{PH} + e^{KN} + e^{PT} + e^{CH} \quad (42)$$

Physical exergy is calculated for fluid flows as follow:

$$e^{PH} = (h - h_o) - T_o(s - s_o) \quad (43)$$

Moreover, chemical exergy is stated for multicomponent mixtures as follow:

$$\bar{e}^{CH} = \sum x_k \bar{e}_k^{CH} + \bar{R} T_0 \sum x_k \ln x_k \quad (44)$$

In the above equation,  $x$  is the molar ratio of the  $k^{\text{th}}$  component, and  $\bar{e}_k^{CH}$  is the standard chemical exergy of the  $k^{\text{th}}$  component.

**4. 1. Desalination System** Enthalpy, and the entropy of water from thermodynamic properties data are applied to calculate the exergy of flows. Salt water enthalpy, and entropy are used to calculate saltwater exergy.

$$s = mf_s s_s + mf_w s_s \quad (45)$$

$$h = mf_s h_s + mf_w h_s \quad (46)$$

In the above equation,  $mf$  denotes the water to salt mass fraction. Since salt water can be considered as diluted mixture, the entropy of salt mixture can be calculated as follows:

$$s_i = s(P, T)_{i, \text{pure}} - R_u \ln x_i \quad (47)$$

#### 5. OPTIMIZATIONS

Due to gradient descent algorithms require satisfactory initial guesses for the parameters, for optimization

process, a heuristic method is employed. In this study, genetic algorithm (GA) as a stochastic optimization method is applied. GA is a population-based optimization method used in searching for the best solution of a given problem based on the concepts of genetics, natural selection and evolution [37].

### 5.1. Objective Functions

**5.1.1. Performance Ratio Maximization** In this study, performance ratio and exergy efficiency of the combined system are the main amount to determine the total efficiency of the system. These parameters have been chosen as objective functions to be maximized.

**5.2. The Decision Parameters** Table 5 presents the decision parameters in the optimization process. Parameters 1–15 are related to METVC and the regenerator boiler; however, Parameters 16–18 are related to the RO unit. Parameter 20 shows the percentage of outlet flow. It is possible to use all or part of the cooling water.

**TABLE 5.** The Minimum and Maximum amount of decision Parameters

No.	Parameter	Unit	Minimum	Maximum
1	Heating steam Temperature ( $T_s$ )	°C	60	70
2	Maximum Brine Water Temperature (TBT)	°C	60	70
3	Motive Steam Pressure ( $P_m$ )	bar	5	45
4	Ejector Compressibility Factor ( $C_r$ )	-	2	4
5	Number of Desalination Steps (N)	-	3	10
6	Condenser Pinch Point ( $\Delta T_{cond}$ )	°C	5	10
7	Tube Length in Each Step ( $L_{eff}$ )	m	4	5
8	Tube Diameter in Each Step ( $d_{eff}$ )	mm	15	40
9	Boiler Pinch Point ( $T_{pp}$ )	°C	5	50
10	Boiler Tubes Length ( $L_{hrsg}$ )	m	10	20
11	Boiler Tubes Diameter ( $d_{hrsg}$ )	mm	25	150
12	Fin density ( $n_f$ )	$m^{-1}$	50	285
13	Fin Thickness ( $t_f$ )	mm	0.9	3
14	Fin Height ( $h_f$ )	mm	13	25
15	Boiler Tubes Pitch ( $p_t$ )	mm	35	600
16	The Pressure of High Pressure Pump [31] ( $P_{hp}$ )	bar	40	82
17	Number of Modules in Pressure Vessel ( $N_m$ )	-	5	8
18	Inlet Water Flow Rate [31] ( $Q_i$ )	$m^3/s$	$8.33 \times 10^{-4}$	0.0045
19	Inlet Water concentration	ppm	36000	45000
20	Percentage of outlet Flow	-	0	1

### 5.3. Constraints

Table 6 lists the constraints in the optimization process. Constraints 1–4 will be applied to both gas turbine cycle and METVC desalination optimization. Equation (5) is associated with maximum concentration of RO desalination brine, while Constraint 6 is related to the temperature constraint of RO feed water [14]. Also, it is assumed that the products of METVC and RO are mixed with each other, to reach a single product. The concentration of single product needs to be less than 250 ppm according to number 7 relation in Table 6.

All mentioned configurations were kept in similar conditions and based on a single objective optimization. The METVC product is limited due to its energy supply from hot exhaust gas of HRSG. However, in terms of RO desalination the required energy is the electricity produced at a power plant. Thus, the optimum solution leads to the noticeable reduction in electricity consumption for RO desalination process. The fact is that the cost of RO product is generally cheaper than product of drinking water in thermal units. So, by choosing cost minimization as the objective of optimization, the optimum solution shows increase of RO production in METVC+RO system. Therefore, the presence of constraints is essential. The optimum water product was 70000 cubic meter per day due to the gas turbine cycle and METVC desalination optimization. This amount was considered as reference and the RO system constraints will be defined based on this value. In this regard, two approaches are considered for optimization:

### 5.4. Optimization Approaches

**5.4.1. First Approach** In this approach, the level of METVC product is constant at 70000 m<sup>3</sup>/day. The level of RO product is 50%, 75%, and 100% of the METVC product. Achieving a high level of production by the METVC unit is the main purpose of this approach.

The levels of the RO products are restricted, and they are 35000, 52500, and 70000 m<sup>3</sup>/day. Hence, the total products of two units are 105000, 122500, and 140000 m<sup>3</sup>/day, respectively.

**TABLE 6.** Physical Restrictions of Optimization Problem

Number	Parameter
1	$T_g2 > 130^\circ C$
2	$T_s - TBT > 3^\circ C$
3	$T_f - T_{cw} > 3^\circ C$
4	$x_N < 70000 \text{ ppm}$
5	$x_{N-RO} < 70000 \text{ ppm}$
6	$T_{f-RO} < 45^\circ C$
7	$x_{P_{tot}} \leq 250 \text{ ppm}$

**5.4.2. Second Approach** In this approach, the level of the METVC product is not constant, and the economic and thermodynamic aspects of the two units are investigated. The total levels of products are considered the limitation, and they are 105000, 122500, and 140000 m<sup>3</sup>/day.

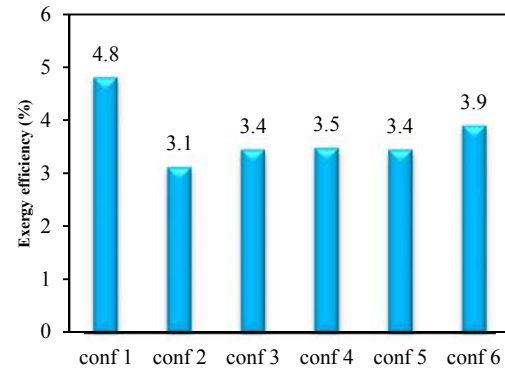
## 6. RESULTS AND DISCUSSIONS

The optimization results of various configurations are presented according to the first and second approaches. As stated in previous sections, the results were based on the PSO algorithm due to the superiority of this algorithm over GA. It is repeated in each stage in order to reach optimal solution. Moreover, the initial population was reported between 2000 and 14000, and the number of repetitions stood at 2000–4000 variable times. The basis of changing the mentioned parameters lies in obtaining more accurate responses due to the high volume of modelling, the high number of decision parameters, and the frequent presence of constraints. Hence, each computing code ranges from almost 60 to 900 minutes. So, long hours were spent to reach optimum solution for each configuration. Due to the mentioned issues, optimal solutions were ensured after reaching the results and processing.

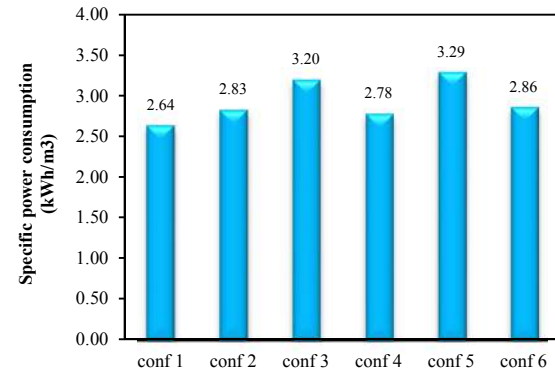
**6.1. First Approach Results** In this section, the exergy efficiency of the METVC+RO system is investigated. Figure 10 shows the exergy efficiency of all configurations in product capacity of 140000 m<sup>3</sup>/day. According to this figure, configurations 1 and 2 have the maximum and minimum exergy efficiency, respectively. As the METVC and RO units have the same product mass flow rate, the product quality is important. So, product exergy is an effective and important factor in exergy efficiency. The higher temperature and lower concentration of the product cause exergy increase. In configuration 1, product temperature and product exergy are higher in the METVC unit and RO unit, respectively. In configuration 2, the final product temperature is higher in the RO unit. However, the heat transfer between the METVC product and RO unit feed water leads to a decrease in temperature and exergy. The RO product temperature in configuration 3 is higher than in configuration 4. In configuration 3, the heat transfer of brine water of METVC has causes a decrease in temperature. The temperatures of the RO product in configurations 5 and 6 are the same as seawater temperature and the exergy efficiency is lower than configuration 1.

Figure 11 shows RO-unit specific power consumption for producing 1 m<sup>3</sup> permeate water for all configurations. In order to recovering pressure of outlet brine, an energy recovery system utilized which

decreases energy consumption of high pressure pump. According to Figure 11, configurations 5 and 1 have the maximum and minimum energy consumption, respectively. The difference of energy consumption is related to pumping energy consumption since the level of product is constant in these configurations. According to Figure 12, the configuration with the minimum recovery rate consumes much feed water and electricity.



**Figure 10.** Exergy efficiency of all configurations in product capacity of 140000 m<sup>3</sup>/day



**Figure 11.** RO-unit-specific power consumption for all configurations

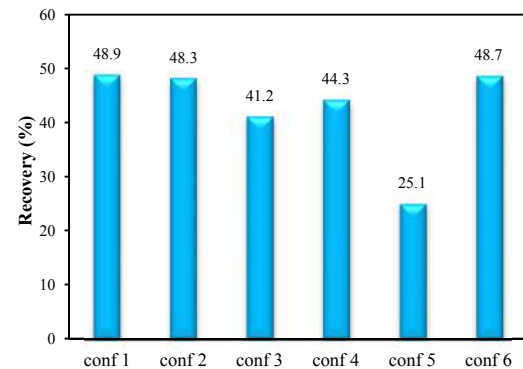


**Figure 12.** Recovery rate of all configurations in product capacity of 140000m<sup>3</sup>/day.

## 6. 2. Second Approach Results

The product constraint is applied to the total number of products of the METVC and RO units. The participation rate of each desalination unit must be determined in the first step. Figures 13 and 14 show the METVC and RO product contribution according to the optimized solution for each configuration in product capacities of 122500 and 140000 m<sup>3</sup>/day, respectively. The maximum METVC contribution is associated with configuration 2 and it is the 44% of the total number of products. The METVC contribution decreases in the other configurations; in configuration 5, it is 20% of total products. Figure 15 presents the METVC coefficient of performance in the first and second approaches. In the second approach, configuration 2 has the maximum coefficient of performance due to the higher contribution of METVC unit.

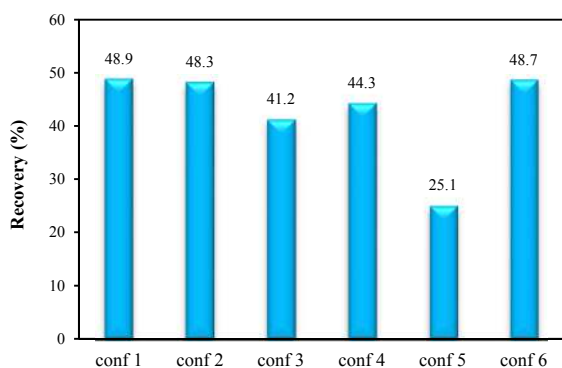


**Figure 13.** Recovery rate of all configurations in product capacity of 140000 m<sup>3</sup>/day

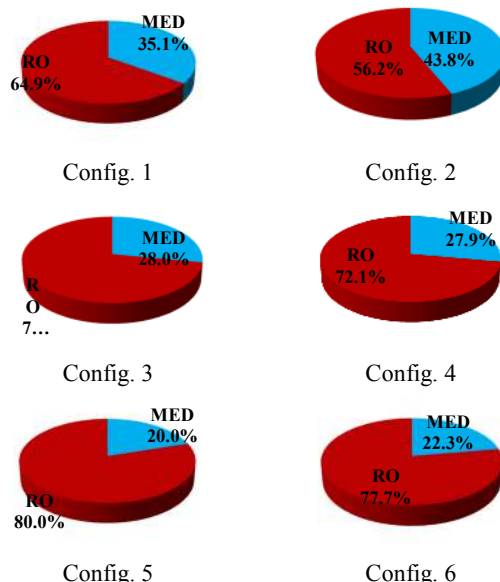


**Figure 14.** METVC and RO contributions to total product at capacity of 140000 m<sup>3</sup>/day

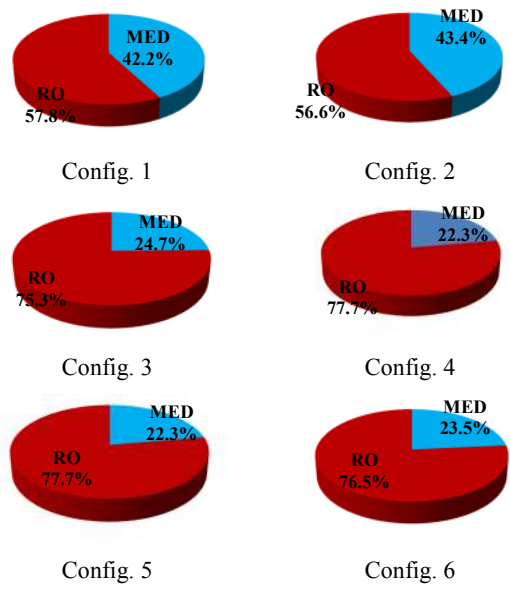


**Figure 15.** METVC and RO contributions to total product at capacity of 122500 m<sup>3</sup>/day

Figures 16 and 17 show the exergy efficiency of all configurations in the first and second optimized approaches at product capacities of 140000 and 122500 m<sup>3</sup>/day, respectively. Configuration 1 has the maximum exergy efficiency to 4.5%. In this configuration, the higher contribution of METVC unit leads to temperature rise in the product of METVC and RO units. So, exergy efficiency increases and there is an acceptable accordance with the results of the first approach. The reduction in contribution of the METVC unit results in a decrease in exergy efficiency.

Figure 18 shows that the configuration 5 has the maximum electricity consumption for producing one cubic meter fresh water owing to a higher level of RO unit feed water supply. The other important factor is the higher RO contribution.

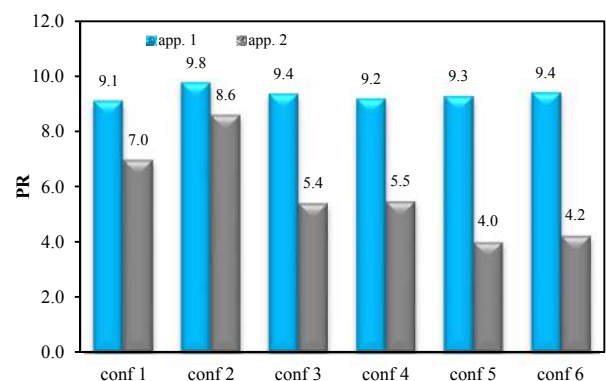


**Figure 16.** The coefficient of performance in METVC unit at capacity of 140000 m<sup>3</sup>/day

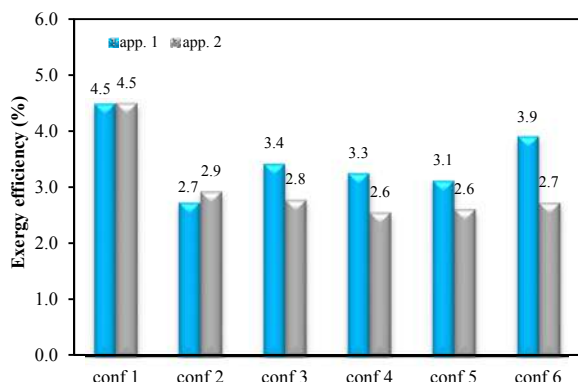


**Figure 17.** Exergy efficiency of all configurations in two optimized approaches at product capacity of 122500 m<sup>3</sup>/day

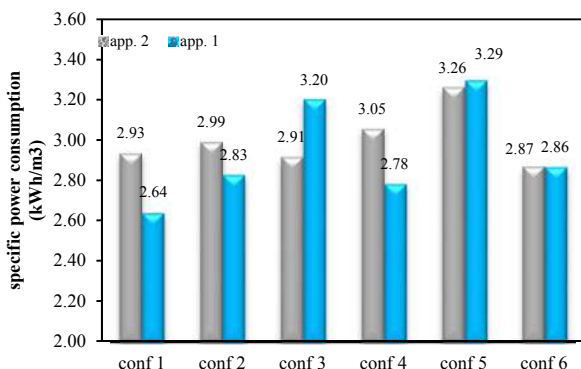


**Figure 18.** Specific power consumption of all configurations of the RO unit.

Giving a better comparison, Table 7 shows the final value of the objective functions obtained through optimization for capacity of 140000 m<sup>3</sup>/day. Also, Table 8 shows the operational conditions of configuration 1 at capacity of 140000 m<sup>3</sup>/day.

**TABLE 7.** Final value of objective functions obtained through optimization for capacity of 140000 m<sup>3</sup>/day

App. no.	Config. no.	$\eta_{ex}$ (%)	PR
App. 1	Config. 1	4.8	9.1
	Config. 2	3.1	9.8
	Config. 3	3.4	9.4
	Config. 4	3.5	9.2
	Config. 5	3.4	9.3
	Config. 6	3.9	9.4
App. 2	Config. 1	4.1	7
	Config. 2	3	8.6
	Config. 3	3.1	5.4
	Config. 4	3.6	5.5
	Config. 5	2.7	4
	Config. 6	3.8	4.2

**TABLE 8.** Operational conditions of configuration 1 at capacity of 140000 m<sup>3</sup>/day

parameter	value
T <sub>cw</sub> (feed of RO) (°C)	39.9
T <sub>s</sub> (oC)	69
T <sub>l</sub> (oC)	66
T <sub>N</sub> (oC)	46
A <sub>tot</sub> (m <sup>2</sup> )	66165
Recovery rate (%)	45.7
PR	9.1
$\eta_{ex}$ (%)	4.8
sE <sub>RO</sub> (kWh/m <sup>3</sup> )	2.6

## 7. CONCLUSION

In this paper, the optimum integration of METVC+RO hybrid desalination and the gas turbine cycle were investigated. It was introduced a comprehensive model for the various sections of the cycle. Furthermore, six different configurations were defined for RO and METVC units. In addition, two optimization approaches were considered for each configuration. In the first approach, the METVC desalination product remained constant at 70000 m<sup>3</sup>/day. So, the METVC is capable to produce higher contribution of essential drinking water where the total product of the two desalination technologies was limited to 105000, 122500, and 140000 m<sup>3</sup>/day. In the second approach, the METVC desalination product was considered unconditional and the product of hybrid desalination system was limited to 105000, 122500, and 140000 m<sup>3</sup>/day. After developing thermodynamic modelling, the results of the first approach show that configurations 1 and 2 have the maximum and minimum exergy efficiency, and configurations 5 and 1 have the maximum and minimum energy consumption, respectively. In the second approach, configurations 1 and 2 have the maximum exergy efficiency and the maximum coefficient of performance, respectively. Therefore, based on the results, the first configuration is chosen as the most optimum system. This configuration possesses the highest exergy in both first and second approaches.

## 8. REFERENCES

1. Seyyedvalilu, M. H., Mohammadkhani, F., and Khalilarya, S., "A Parametric Study on Exergy and Exergoeconomic Analysis of a Diesel Engine based Combined Heat and Power System", *International Journal of Engineering - Transactions A: Basics*, Vol. 28, No. 4, (2015), 608–617.
2. Wang, Y. and Lior, N., "Performance analysis of combined humidified gas turbine power generation and multi-effect thermal

- vapor compression desalination systems — Part 1: The desalination unit and its combination with a steam-injected gas turbine power system”, *Desalination*, Vol. 196, No. 1–3, (2006), 84–104.
3. Halal, A.M., El-Nashar, A.M., Al-Katheeri, E., and Al-Malek, S., “Optimal design of hybrid RO/MSF desalination plants Part I: Modeling and algorithms”, *Desalination*, Vol. 154, No. 1, (2003), 43–66.
  4. Kazemian, M. E., Ebrahimi-Nejad, S., and Jaafarian, M., “Experimental Investigation of Energy Consumption and Performance of Reverse Osmosis Desalination using Design of Experiments Method”, *International Journal of Engineering - Transactions A: Basics*, Vol. 31, No. 1, (2017), 79–87.
  5. Salimi, M., and Amidpour, M., “Modeling, simulation, parametric study and economic assessment of reciprocating internal combustion engine integrated with multi-effect desalination unit”, *Energy Conversion and Management*, Vol. 138, (2017), 299–311.
  6. Elsayed, M. L., Mesalhy, O., Mohammed, R.H., and Chow, L.C., “Exergy and thermo-economic analysis for MED-TVC desalination systems”, *Desalination*, Vol. 447, (2018), 29–42.
  7. Khalilzadeh, S. and Hossein Nezhad, A., “Utilization of waste heat of a high-capacity wind turbine in multi effect distillation desalination: Energy, exergy and thermoeconomic analysis”, *Desalination*, Vol. 439, (2018), 119–137.
  8. Ihm, S., Al-Najdi, O.Y., Hamed, O.A., Jun, G., and Chung, H., “Energy cost comparison between MSF, MED and SWRO: Case studies for dual purpose plants”, *Desalination*, Vol. 397, (2016), 116–125.
  9. Zak, G. M., and Mitsos, A., “Hybrid thermal-thermal desalination structures”, *Desalination and Water Treatment*, Vol. 52, No. 16–18, (2014), 2905–2919.
  10. Alamolhoda, F., KouhiKamali, R., and Asgari, M., “Parametric simulation of MED–TVC units in operation”, *Desalination and Water Treatment*, Vol. 57, No. 22, (2016), 10232–10245.
  11. Zhao, D., Liu, T., Xue, J., Li, S., Li, C., Liu, W., Zhang, H., and Wang, Y., “A lab-scale MED dealing with salinity wastewater: the study of optimal operation schemes and parameters”, *Desalination and Water Treatment*, Vol. 57, No. 25, (2016), 11721–11728.
  12. Catrini, P., Cipollina, A., Micale, G., Piacentino, A., and Tamburini, A., “Exergy analysis and thermoeconomic cost accounting of a Combined Heat and Power steam cycle integrated with a Multi Effect Distillation-Thermal Vapour Compression desalination plant”, *Energy Conversion and Management*, Vol. 149, (2017), 950–965.
  13. Alelyani, S. M., Fette, N.W., Stechel, E.B., Doron, P., and Phelan, P.E., “Techno-economic analysis of combined ammonia-water absorption refrigeration and desalination”, *Energy Conversion and Management*, Vol. 143, (2017), 493–504.
  14. Ghafuoryan, M. M., Shakib, S. E., and Dastjerdi, F. T., “Modeling and optimizing of a combined CHP system, compression chiller and reverse osmosis plant (CHP + C + W) in two strategies of connections with grid”, *Journal of the Brazilian Society of Mechanical Sciences and Engineering*, Vol. 37, No. 6, (2015), 1751–1763.
  15. Awerbuch, L., Van der Mast, V., and Soo-Hoo, R., “Hybrid desalting systems - a new alternative”, *Desalination*, Vol. 64, (1987), 51–63.
  16. Altmann, T., “A new power and water cogeneration concept with the application of reverse osmosis desalination”, *Desalination*, Vol. 114, No. 2, (1997), 139–144.
  17. Al-Mutaz, I. S., “A comparative study of RO and MSF desalination plants”, *Desalination*, Vol. 106, No. 1–3, (1996), 99–106.
  18. La Bar, M., Schleicher Jr, R., Loh, G., and Walters, A., “Power and water co-production feasibility study for Florida power & light power plants”, *Desalination*, Vol. 88, No. 1–3, (1992), 267–277.
  19. Kamal, I., “An assessment of desalination technology for the Rosarito Repowering Project”, *Desalination*, Vol. 102, No. 1–3, (1995), 269–278.
  20. Muginstein, A., Cohen, Y., Levin, L., and Frant, S., “Production of desalinated water and electricity in a dual-purpose plant operating in a dispatchable electricity system — technoeconomical analysis”, *Desalination*, Vol. 156, No. 1–3, (2003), 361–366.
  21. Cardona, E., Piacentino, A., and Marchese, F., “Performance evaluation of CHP hybrid seawater desalination plants”, *Desalination*, Vol. 205, No. 1–3, (2007), 1–14.
  22. Messineo, A. and Marchese, F., “Performance evaluation of hybrid RO/MEE systems powered by a WTE plant”, *Desalination*, Vol. 229, No. 1–3, (2008), 82–93.
  23. Zak, G. M., Ghobeity, A., Sharqawy, M.H., and Mitsos, A., “A review of hybrid desalination systems for co-production of power and water: analyses, methods, and considerations”, *Desalination and Water Treatment*, Vol. 51, No. 28–30, (2013), 5381–5401.
  24. Iaquaniello, G., Salladini, A., Mari, A., Mabrouk, A., and Fath, H., “Concentrating solar power (CSP) system integrated with MED–RO hybrid desalination”, *Desalination*, Vol. 336, (2014), 121–128.
  25. Mokhtari, H., Sepahvand, M., and fasihfar, A., “Thermoeconomic and exergy analysis in using hybrid systems (GT + MED + RO) for desalination of brackish water in Persian Gulf”, *Desalination*, Vol. 399, (2016), 1–15.
  26. Sadri, S., Ameri, M., and Haghghi Khoshkho, R., “Multi-objective optimization of MED–TVC-RO hybrid desalination system based on the irreversibility concept”, *Desalination*, Vol. 402, (2017), 97–108.
  27. Shakib, S. E., Amidpour, M., and Aghanajafi, C., “A new approach for process optimization of a METVC desalination system”, *Desalination and Water Treatment*, Vol. 37, No. 1–3, (2012), 84–96.
  28. Shakib, S. E., Amidpour, M., and Aghanajafi, C., “Simulation and optimization of multi effect desalination coupled to a gas turbine plant with HRSG consideration”, *Desalination*, Vol. 285, (2012), 366–376.
  29. Esmaeli, A., Keshavarz M, P., Shakib, S.E., and Amidpour, M., “Applying different optimization approaches to achieve optimal configuration of a dual pressure heat recovery steam generator”, *International Journal of Energy Research*, Vol. 37, No. 12, (2013), 1440–1452.
  30. Power R.B., Steam jet ejectors for the process industries. [Glossary included], New York (United States); McGraw-Hill, (1994).
  31. Shakouri, M., Ghadamian, H., and Sheikholeslami, R., “Optimal model for multi effect desalination system integrated with gas turbine”, *Desalination*, Vol. 260, No. 1–3, (2010), 254–263.
  32. Kaghazchi, T., Mehri, M., Ravanchi, M.T., and Kargari, A., “A mathematical modeling of two industrial seawater desalination plants in the Persian Gulf region”, *Desalination*, Vol. 252, No. 1–3, (2010), 135–142.
  33. Dickson, J. M. and Mehdizadeh, H., “Overview of Reverse Osmosis for Chemical EngineersPart 1, Fundamentals of Membrane Mass Transfer”, *International Journal of Engineering*, Vol. 1, No. 4, (1988), 163–180.
  34. Avlonitis, S. A., Pappas, M., and Moutsidis, K., “A unified model for the detailed investigation of membrane modules and RO plants performance”, *Desalination*, Vol. 203, No. 1–3, (2007), 218–228.

35. Safar, M., Jafar, M., Abdel-Jawad, M., and Bou-Hamad, S., "Standardization of RO membrane performance", *Desalination*, Vol. 118, No. 1–3, (1998), 13–21.
36. Bejan, A., Tsatsaronis, G., Moran, M. and Moran, M.J., Thermal design and optimization, John Wiley & Sons, (1996).
37. Holland, J., Adaptation in natural and artificial systems: an introductory analysis with application to biology, Control and Artificial Intelligence, Ann Arbor, MI: University of Michigan Press, (1975).

## Various Approaches to Thermodynamic Optimization of a Hybrid Multi-effect Evaporation with Thermal Vapour Compression and Reverse Osmosis Desalination System Integrated to a Gas Turbine Power Plant

S. E. Shakiba<sup>a</sup>, M. Amidpour<sup>b</sup>, A. Esmaielib, M. Boghrati<sup>a</sup>, M. M. Ghafurian<sup>c</sup>

<sup>a</sup> Department of Mechanical Engineering, Bozorgmehr University of Qaenat, Qaen, Iran

<sup>b</sup> Faculty of Mechanical Engineering, K.N. Toosi University of Technology, Tehran, Iran

<sup>c</sup> Department of Mechanical Engineering, Faculty of Engineering, Ferdowsi University of Mashhad, Mashhad, Iran

چکیده

### PAPER INFO

#### Paper history:

Received 14 December 2018

Received in revised form 30 January 2019

Accepted 07 March 2019

#### Keywords:

Optimal Design

Multi-effect Evaporation with Thermal

Vapour Compression

Reverse Osmosis

Desalination

Thermodynamic Approach

این مقاله به شبیه‌سازی سیستم آب‌شیرین کن ترکیبی شامل آب‌شیرین کن تبخیری چند مرحله با تراکم گرمایی بخار و آب شیرین اسمز معکوس می‌پردازد. سیستم آب‌شیرین کن ترکیبی مورد نظر از طریق بویلر بازیاب به یک نیروگاه توربین گازی متصل است. ابتدا مدل ترمودینامیکی جامع از بویلر بازیاب، آب‌شیرین کن تبخیری چند مرحله‌ای و آب‌شیرین کن اسمز معکوس توسعه یافت تا بتوان توسط آن رفتار گرمایی آب‌شیرین کن ترکیبی را پیش‌بینی نمود. بسته به نحوه اتصال دو آب‌شیرین کن مذکور که به ارتباط بین جریان‌های ورودی و خروجی آنها ارتباط دارد شش چیدمان برای سیستم آب‌شیرین کن ترکیبی پیشنهاد شد. این شش چیدمان با دو رویکرد مختلف مورد مطالعه قرار گرفت. در رویکرد اول ظرفیت تولید آب شیرین در آب‌شیرین کن گرمایی چند مرحله ثابت و به مقدار ۷۰۰۰۰ مترمکعب در روز در نظر گرفته شد. در واقع در این رویکرد از کل پتانسیل گرمایی گازهای داغ خروجی از توربین گاز برای تولید آب شیرین استفاده شد. در رویکرد دوم، ظرفیت تولید آب‌شیرین کن گرمایی چند مرحله‌ای متغیر در نظر گرفته شد و محدودیت تولید آب شیرین بر مجموع تولید دو آب‌شیرین کن مورد مطالعه به عنوان قید بهینه‌سازی اعمال شد. نتایج نشان داد در هر دو رویکرد چیدمان اول (چیدمانی که در آن از آب خنک کن آب‌شیرین کن گرمایی به عنوان آب تغذیه واحد اسمز معکوس استفاده شده است) کمترین مصرف انرژی و بالاترین راندمان اگزرسی را داراست.

doi: 10.5829/ije.2019.32.05b.20